DOI: 10.23968/2500-0055-2022-7-2-66-78

MODELING NON-STATIONARY TEMPERATURE FIELDS WHEN CONSTRUCTING MASS CAST-IN-SITU REINFORCED-CONCRETE FOUNDATION SLABS

Anton Chepurnenko*, Grigory Nesvetaev, Yuliya Koryanova

Don State Technical University
Gagarin square 1, Rostov-on-Don, Russia

*Corresponding author: anton_chepurnenk@mail.ru

Abstract

Introduction: Due to hydration heating and heat exchange with the environment during hardening, mass cast-in-situ reinforced-concrete structures exhibit non-uniform heating, which can result in early cracking and make the structures unsuitable for further use. One of the main risk factors for early cracking is the temperature difference between the center and the surface of the structure. **Purpose of the study:** We aimed to study how such factors as the ratio of dimensions, heat transfer conditions on the surfaces, concrete recipe, pauses during concreting and their duration affect the maximum temperature difference between the center and the surface of the structure. **Methods:** In the course of the study, we applied finite element modeling in one-dimensional and three-dimensional cases using the software in the MATLAB environment that we developed earlier. **Results:** We established that the most significant risk factors for early cracking are heat exchange conditions on the top surface, structural thickness, and the heat release rate of concrete. Verification and validation of the model were performed based on experimental data and by comparing it with a numerical solution in the ANSYS software.

Keywords

Mass reinforced-concrete structures, foundation slab, cracking, temperature field, finite element method, internal heat sources.

Introduction

The issue of cracking in hardening reinforced-concrete structures has been existing as long as reinforced concrete itself. It was first encountered at the beginning of the 20th century during dam concreting (Javanmardi and Léger, 2005; Van Breugel, 1998).

Due to non-uniform temperature distribution throughout the volume as well as concrete shrinkage deformations, an internal stress field may form in mass cast-in-situ structures, exceeding the strength characteristics of concrete at the stage of its structure formation. That may result in early cracking followed by crack development, thus not only negatively affecting the performance of the structure but bringing its operation into question (Castilho et al., 2018; Chuc et al., 2018; Korotchenko et al., 2016).

One of the main risk factors for early cracking is the temperature difference between the center and the surface of the structure (Klemczak and Knoppik-Wróbel, 2011). Table 1 shows the allowable temperature difference between the center and the surface of the structure *ΔT* and the allowable temperature gradient *ΔT/Δh* (based on the use of some available sources).

Table 1. Allowable temperature parameters during the construction of mass cast-in-situ reinforced-concrete structures

Reference	Indicator	Value
Rahimi and Noorzaei, 2011	ΔT	< 20°C
TCXDVN 305:2004	$\Delta T/\Delta h$	< 50°C/m
Bofang, 2014	ΔT	19…16°C[1]
CIRIA C600	ΔT	$\Delta T < \frac{3.7\varepsilon}{\alpha}$ [2]
R NOSTROY 2.6.17-2016	ΔT	9…16°C[3]

Notes: 1 — at a block length of 31–40 m and a height/length ratio of less than 0.1; 2 — where ε is the ultimate tensile strain of concrete, α is the coefficient of thermal expansion of concrete; 3 — depending on the ultimate strength of concrete and reinforcement ratio.

The temperature origin of cracks in cast-in-situ structures at the stage of construction was first pointed out by the Soviet scientist V. S. Lukyanov in the 1930s. At the time, it was impossible to obtain a direct solution to the problem of calculating temperature fields by integrating differential equations, and he designed a device to predict temperature conditions based on the hydraulic analogy (Lukyanov, 1935).

With modern computing systems, we can easily obtain a direct solution to the differential equation for thermal conductivity, including in a three-dimensional case. Numerous works addressed the calculation of temperature fields at the stage of manufacturing mass cast-in-situ structures. For instance, Kuriakose et al. (2016) solved the problem of calculating the temperature field, considering the relationship between the thermal conductivity coefficient of concrete and the degree of hydration. Nguyen and Luu (2019) proposed a method to reduce the temperature difference between the center and the surface of the structure by surface insulation. They carried out modeling using the Midas Civil software. Xu et al. (2019) performed finite element modeling of cracking prevention in concrete using water cooling in the ABAQUS environment. This problem was also considered by Nguyen et al. (2019) as well as Tasri and Susilawati (2019). Klemczak et al. (2017) studied the influence of concrete composition on the thermophysical properties of concrete and the risk of early cracking using finite element analysis. A similar problem was solved by Van Lam et al. (2018). Xie et al. (2020) proposed an interval finite element method to calculate temperature fields. Using this method, it is possible to perform analysis under the influence of multiple uncertainties, e.g., environmental temperature, material properties, pouring and pipe cooling technology. Havlásek et al. (2017) proposed a weakly-coupled thermo-mechanical model for early-age concrete with an affinity-based hydration model for the thermal part, taking into account concrete mix design, cement type, and thermal boundary conditions. Abeka et al. (2017) performed experimental and numerical investigations of thermal effects on mass concrete structures in the tropics.

Długosz et al. (2017) presented evolutionary computation procedures to identify thermophysical properties in hardening mass cast-in-situ reinforced-concrete structures Fairbairn et al. (2004) used genetic algorithms for the optimization of mass cast-in-situ structures. Kuryłowicz-Cudowska (2019) addressed the modeling of temperature fields in cast-in-situ reinforced-concrete bridge decks. When studying the temperature fields of mass cast-in-situ structures, Zhang et al. (2020) introduced the temperature influence factor for the heat release rate.

In all the papers mentioned above, during temperature field modeling, it was assumed that the structure is made in one step. In real practice, concreting can take considerable time and may involve pauses. Besides, there are several other factors affecting non-uniform temperature distribution through the thickness of the structure. They affect the likelihood of early cracking to different extents. We aimed to study how such factors as the ratio of dimensions, heat transfer conditions on the surfaces, concrete recipe, pauses during concreting and their duration affect the maximum temperature difference between the center and the surface of the structure.

Methods

It is known that in the case of structures made of isotropic materials, the non-stationary problem of thermal conductivity with account for internal heat sources reduces to the following differential equation (Semenov, 2019):

$$\lambda\left(\frac{\partial^2 T}{\partial x^2}+\frac{\partial^2 T}{\partial y^2}+\frac{\partial^2 T}{\partial z^2}\right)+Q=\rho c\frac{\partial T}{\partial t}, \tag{1}$$

where λ — the coefficient of thermal conductivity, T — temperature, Q — heat release rate, ρ — material density, c — specific heat capacity, t — time.

When modeling heat release in foundation slabs, we will consider boundary conditions of two types. If there is convective heat exchange with the environment on any surface of the foundation, then the boundary conditions can be written in the following form:

$$\lambda\frac{\partial T}{\partial n}+h\left(T-T_\infty\right)=0, \tag{2}$$

where n — the normal to the surface, h — the heat transfer coefficient, T_∞— the environmental temperature.

The foundation is modeled together with the soil mass. For soil points at a sufficient distance from the foundation, the temperature can be considered set as follows:

$$T_g\left(t\right)=f\left(t\right). \tag{3}$$

Foundation heating from solar radiation is disregarded. To solve the non-stationary problem of thermal conductivity, we developed a program based on the finite element method in the MATLAB environment. When temperature fields are calculated with the use of the finite element method, the solution to Eq. (1) with boundary conditions (2), (3) reduces to finding the minimum of the following functional (Segerlind, 1984):

$$\chi=\int_V\frac{1}{2}\left[\begin{array}{c}\lambda\left(\left(\frac{\partial T}{\partial x}\right)^2+\left(\frac{\partial T}{\partial y}\right)^2+\left(\frac{\partial T}{\partial z}\right)^2\right)- \\ 2\left(Q-\rho c\frac{\partial T}{\partial t}\right)T\end{array}\right]dV+ \tag{4}$$

$$\frac{1}{2}\int_S h\left(T^2-2TT_\infty+T_\infty^2\right)dS,$$

where V — the volume of the body, S — the area of the surface with convective heat exchange on it.

During calculations, we used finite elements in the form of parallelepipeds. When the temperature is approximated within an element:

$$T(x,y,z)=[N]\{T\}, \tag{5}$$

where [N] — the shape function matrix, {**T**} — the vector of nodal temperature values, then after minimizing functional (4), the problem reduces to the following system of differential equations:

$$[C]\frac{\partial\{\mathrm{T}\}}{\partial t}+[K]\{T\}+\{F\}=0, \tag{6}$$

where [C] — the damping matrix, [K] — the thermal conductivity matrix, {**F**} — the load vector.

For each finite element, the matrices [C], [K], {**F**} can be represented by integrals:

$$\left[C^{(e)}\right]=\int_V \rho c[N]^T[N]dV,\left[K^{(e)}\right]= \int_V [B]^T[D][B]dV+\int_S h[N]^T[N]dS, \tag{7}$$
$$\left[F^{(e)}\right]=-\int_V Q[N]^T dV-\int_S hT_\infty[N]^T dS.$$

where [B] — the shape function gradient matrix, $[D]=\begin{bmatrix}\lambda & 0 & 0\\ 0 & \lambda & 0\\ 0 & 0 & \lambda\end{bmatrix}$ in the case of isotropic material.

There are various difference schemes to solve systems of the form (6). With the simplest approximation of the time derivative:

$$\frac{\partial\{T\}}{\partial t}=\frac{\{T_i\}-\{T_{i-1}\}}{\Delta t}, \tag{8}$$

at the ith step, the system of differential equations (6) reduces to the following system of linear algebraic equations:

$$\left([K]+\frac{[C]}{\Delta t}\right)\{T_i\}=\frac{[C]}{\Delta t}\{T_{i-1}\}-\{F\}. \tag{9}$$

In this study, foundation slabs rectangular in plan were considered. Due to symmetry, only a quarter of the structure was modeled. Fig. 1 shows its analytical model.

On the top surface of the foundation (yellow), boundary conditions (2) with the heat transfer coefficient h_1 are accepted. On the side surfaces of the foundation covered with the formwork (green), boundary conditions (2) with the heat transfer coefficient h_2 are accepted. On the top surface of the soil (orange), boundary conditions (2) with the heat transfer coefficient h_3 are accepted. On the side surfaces of the soil (blue) and on its bottom surface, the temperature is considered to be set.

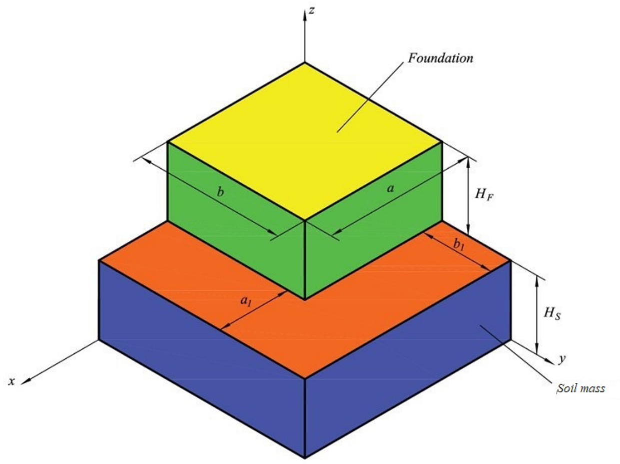

Fig. 1. Analytical model

In mass cast-in-situ foundations of constant thickness, at points at a sufficient distance from the edges, temperature distribution does not depend on the *x* and *y* coordinates, i.e., instead of a three-dimensional thermal conductivity problem, a one-dimensional problem can be solved with the use of the following equation:

$$\lambda\frac{\partial^2 T}{\partial z^2}+Q=\rho c\frac{\partial T}{\partial t}. \tag{10}$$

The use of a one-dimensional model instead of a three-dimensional one significantly saves computing time when conducting parametric studies on the influence of various variables responsible for heat exchange. The possibility of using a one-dimensional formulation instead of a three-dimensional one will be discussed in the next section.

We measured the rate of heat release Q during hardening for five concrete compositions, which differed in cement hydration heat values. Fig. 2 presents corresponding $Q(t)$ graphs.

Results

To validate the model, we first performed tests based on experimental data. Let us present the results of the analysis for a mass structure, involving in-situ temperature measurements and finite element modeling in the program that we developed earlier. Table 2 shows those calculated characteristics.

Table 2. Characteristics of the structure under consideration

Dimensions, m	Temperature, °C			Heat transfer coefficient, W/(m²·°C)		
	concrete mix during laying	air	soil	h_1	h_2	h_3
28.7 × 4 × 2	15	8...13	8	4.5	2	25

The thermophysical properties of concrete: λ = 2.67 W/(m·°C), ρ = 2500 kg/m³, c = 1000 J/(kg·°C). The thermophysical properties of the soil mass: λ = 1.5 W/(m·°C), ρ = 1600 kg/m³, c = 1875 J/(kg·°C). The composition of concrete corresponds to curve 2 in Fig. 2.

Fig. 3 shows data on temperature changes in the center and on the top surface of the structure at x = 0 and y = 0, obtained as a result of in-situ measurements (dashed lines) and modeling with the use of the finite element method (solid lines).

The experimental results are in good agreement with the numerical calculations. The deviation of the results is probably due to the fact that the thermophysical properties of concrete were taken constant in time and their dependence on the degree of cement hydration was not considered. It should also be noted that the results of the analysis with the use of the three-dimensional and one-dimensional models for the center of the structure differ insignificantly.

Our objective was to establish ratios between the dimensions of the structure in plan and its height, at which conditions on the side surfaces do not affect the maximum temperature difference through the thickness of the structure. It is possible

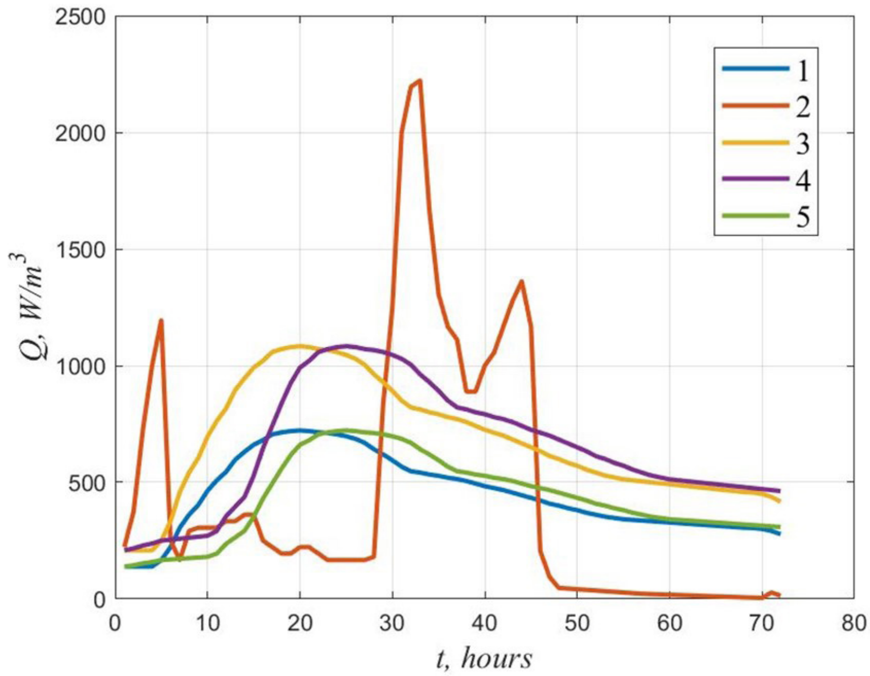

Fig. 2. Rate of heat release $Q(t)$ for various concrete compositions

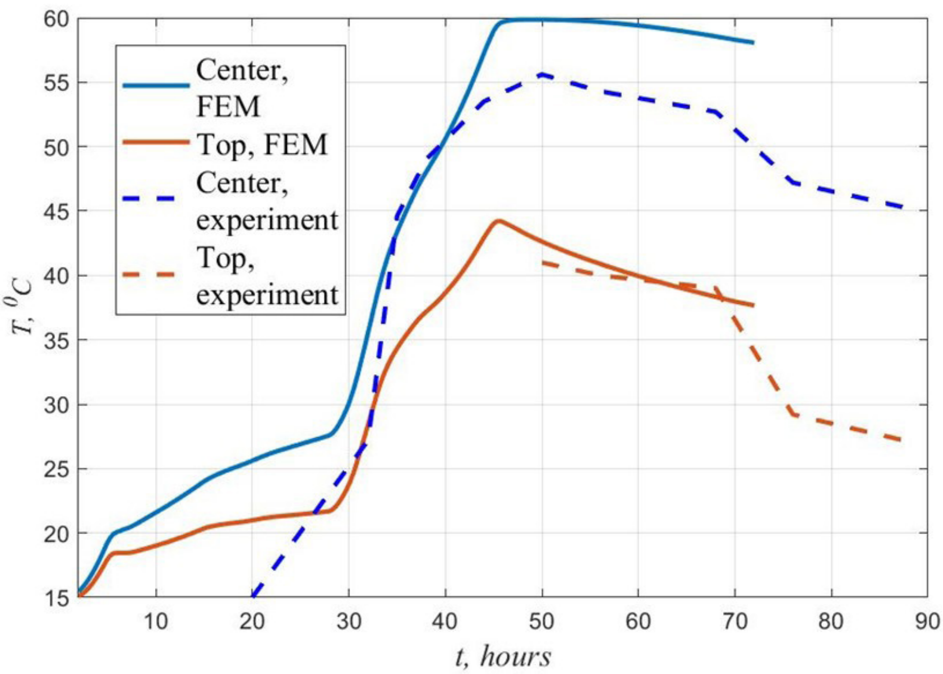

Fig. 3. Temperature vs. concrete hardening time

to use a one-dimensional model instead of a three-dimensional one for calculations. The parametric study was carried out based on the same initial data as in Table 2, except for the dimensions and the heat transfer coefficient h_2 on the side surfaces. The thickness of the structure was assumed to be constant (H_F = 2 m). For simplicity, it was taken that $a = b$, and the ratio a/H_F varied. For the coefficient h_2, the calculations were performed at the following two values: h_2 = 2 W/(m²×°C), which corresponds to the insulated formwork, and h_2 = 25 W/(m²×°C), which corresponds to the exposed surface left for drying.

Fig. 4 presents the maximum temperature difference ΔT between the center and the top surface of the structure vs. time curves. The graphs show that already at a/H_F = 1.5, the influence of conditions on the side surfaces becomes insignificant, and the one-dimensional model makes it possible to obtain acceptable results. A similar analysis was carried out at smaller foundation thicknesses: H_F= 1 m and H_F= 0.7 m. The corresponding graphs are shown in Figs. 5 and 6. At H_F= 1 m, a one-dimensional model can be used if $a/H_F \geq 3$, and at H_F= 0.7 m, a one-dimensional model can be used if $a/H_F \geq 4$.

Next, we studied the heat exchange conditions on the top surface of the foundation. The parametric study was carried out based on the same initial data as in Table 2, except for the coefficient h_1, which varied. Fig. 7 presents changes in the maximum temperature difference between the center and the top surface of the structure in time at various h_1 values. It shows that with an increase in the heat transfer coefficient, the maximum temperature difference increases as well. A similar pattern was observed under other environmental conditions as well as other foundation dimensions. Thus, to reduce the difference between the center and the top surface of the structure, it is reasonable to reduce heat transfer on the top surface.

We also analyzed the influence of concrete composition on the maximum temperature difference between the center and the surface of the structure. The calculations were carried out based on the same initial data as in Table 2 for concrete compositions 1–5 in Fig. 2. Fig. 8 presents changes in the maximum temperature difference between the center and the surface of the structure in time. It shows that the use of concretes with low hydration heat (compositions 1, 2, 5) is an effective way to reduce the ΔT value.

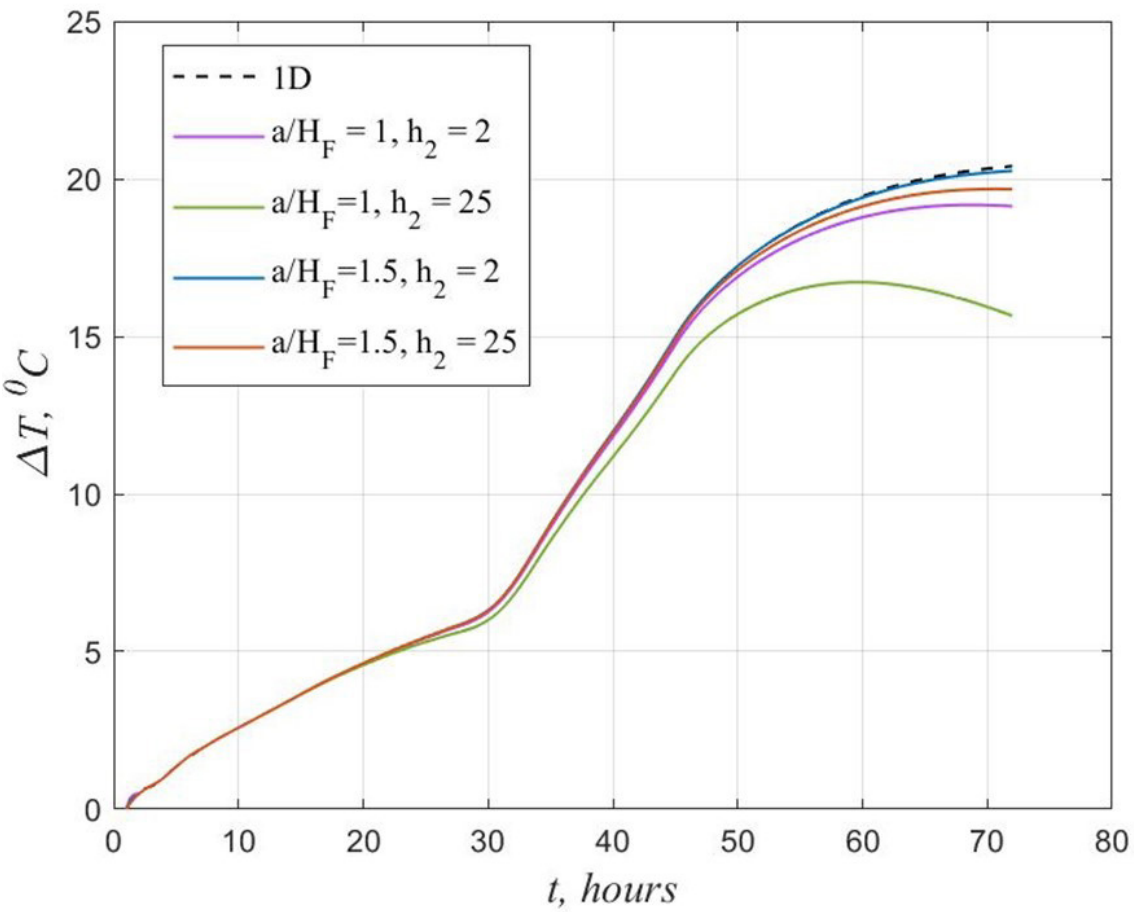

Fig. 4. Relationship between the temperature difference (between the center and the top surface of the structure) and the ratio of the foundation dimensions and conditions on the side surfaces at H_F= 2 m

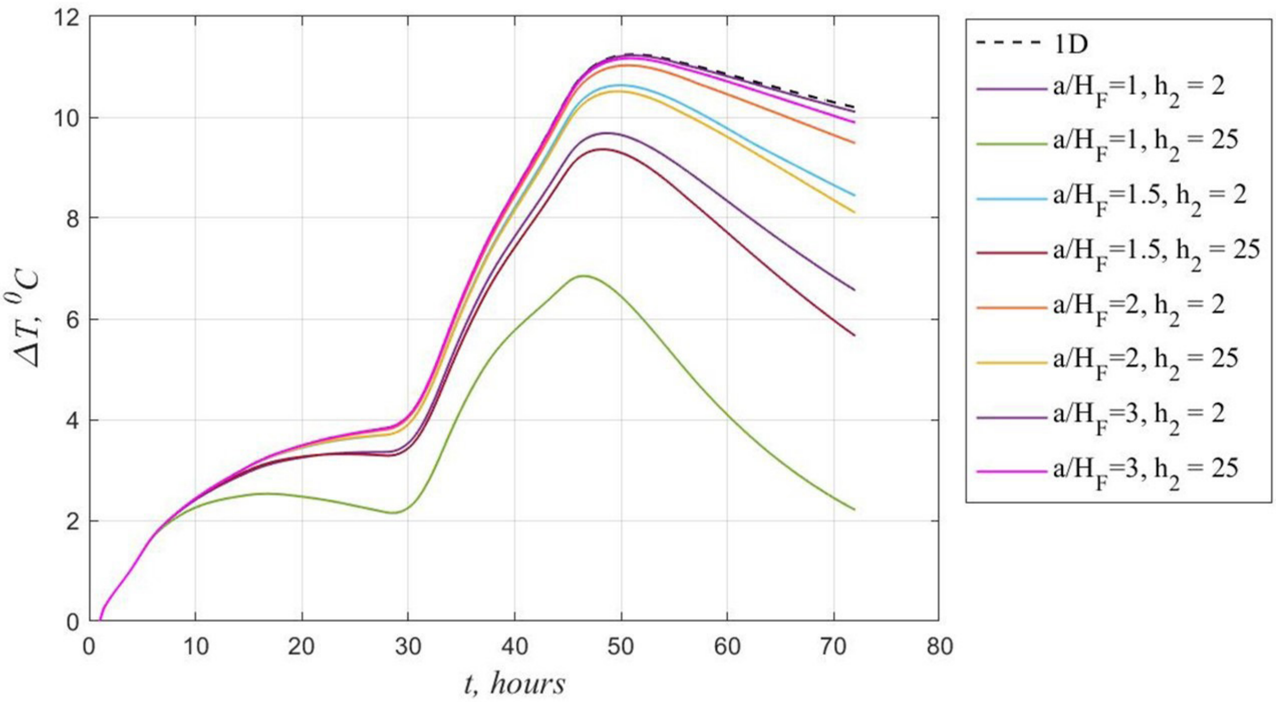

Fig. 5. Relationship between the temperature difference (between the center and the top surface of the structure) and the ratio of the foundation dimensions and conditions on the side surfaces at H_F= 1 m

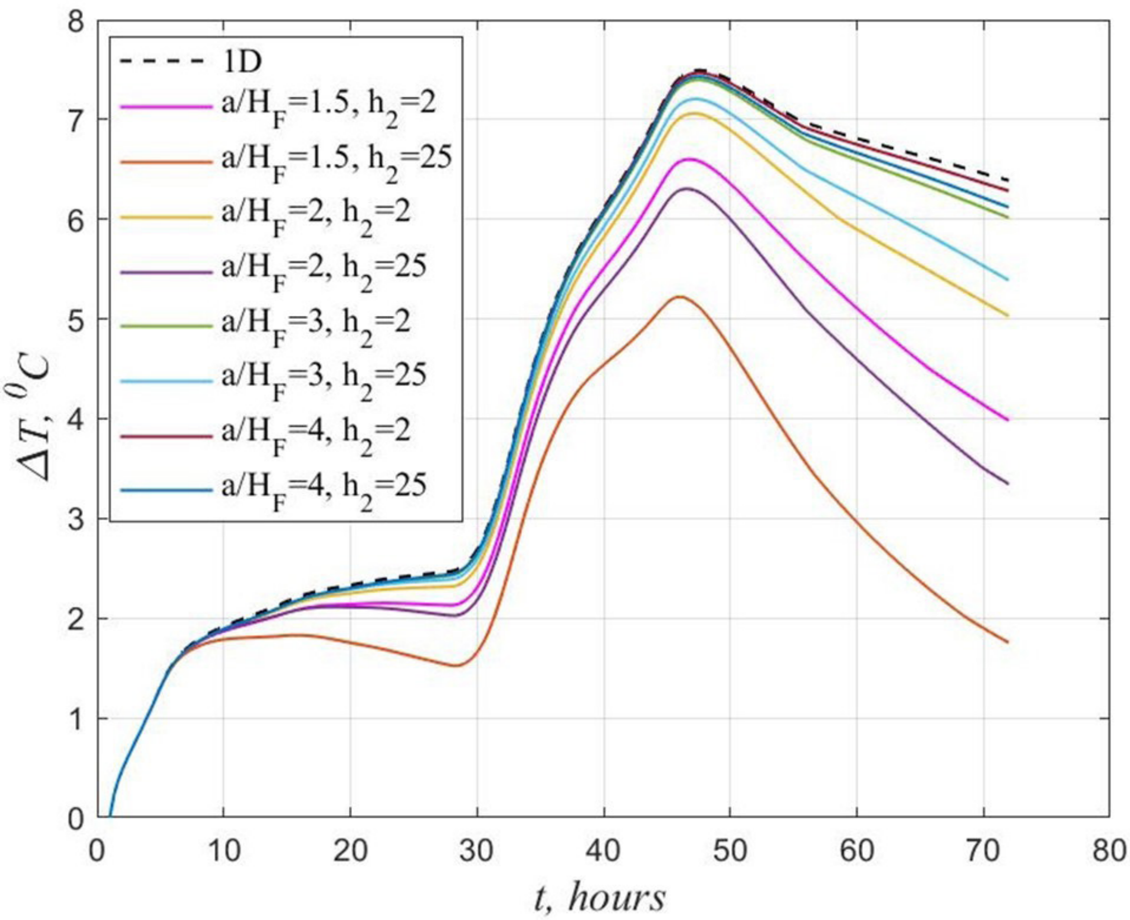

Fig. 6. Relationship between the temperature difference (between the center and the top surface of the structure) and the ratio of the foundation dimensions and conditions on the side surfaces at H_F= 0.7 m

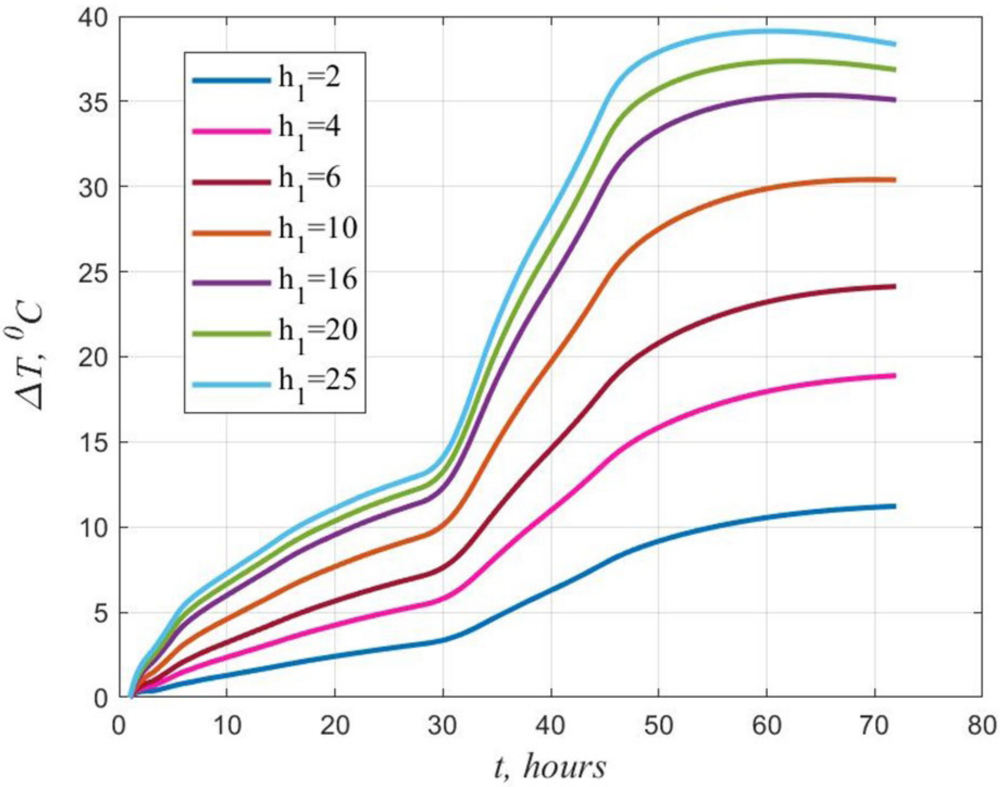

Fig. 7. Relationship between the temperature difference and the heat transfer coefficient on the top surface

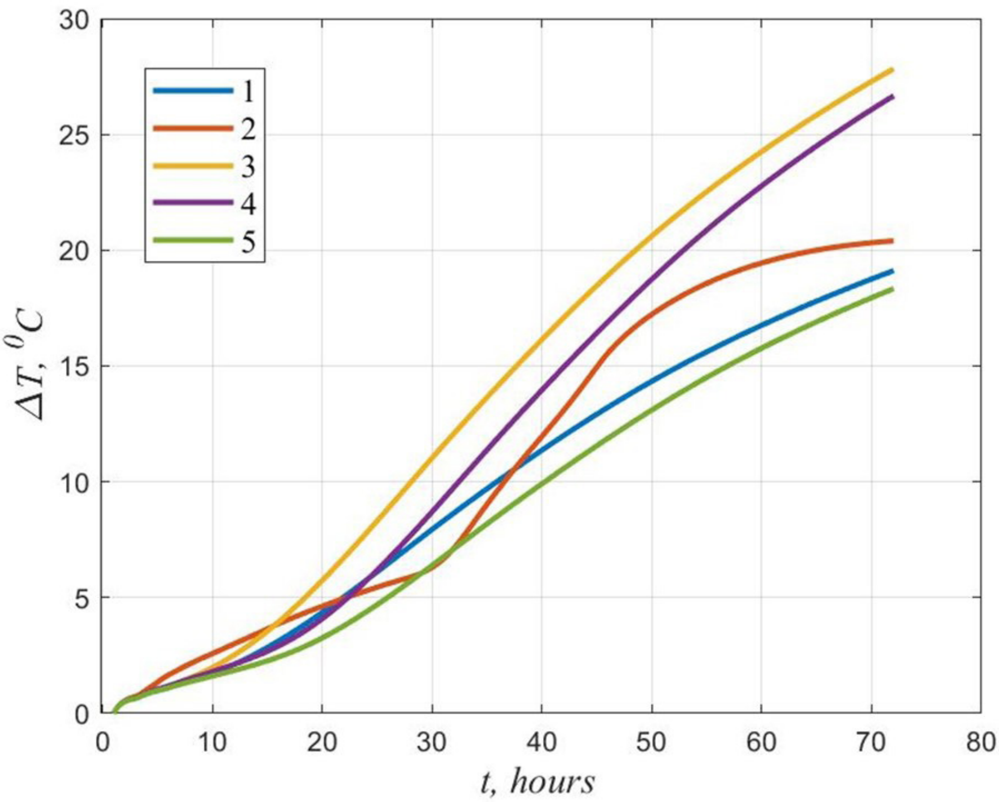

Fig. 8. Relationship between the maximum temperature difference and concrete composition

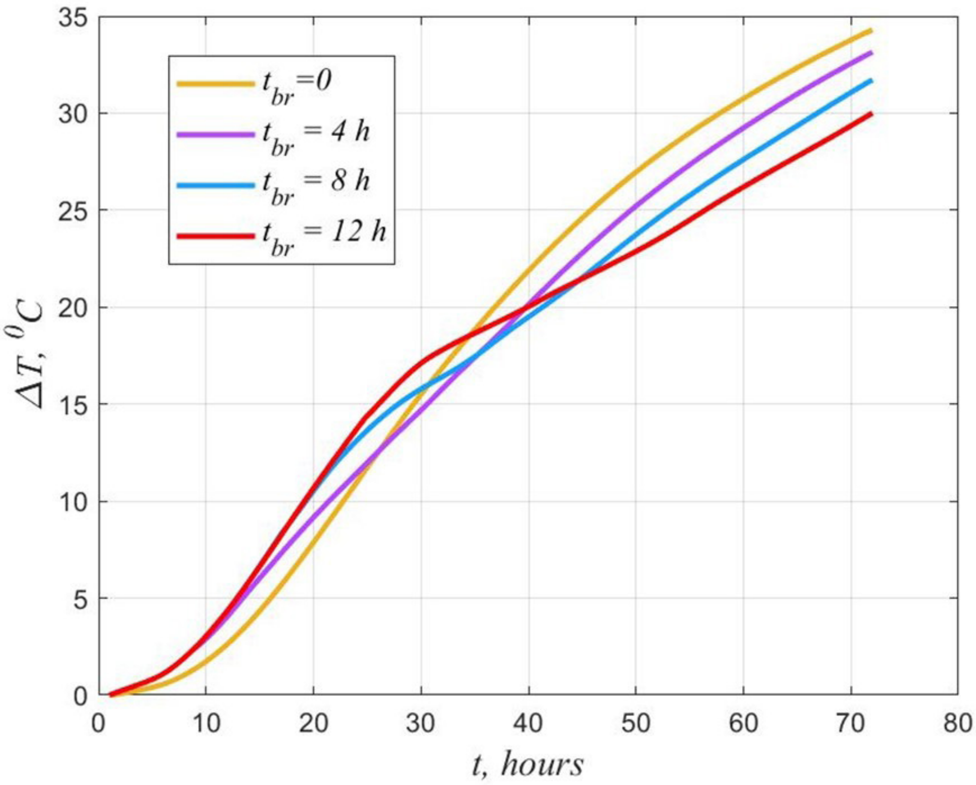

Fig. 9. Changes in the difference between the maximum temperature and the temperature of the top surface in time at different values of t_{br}.

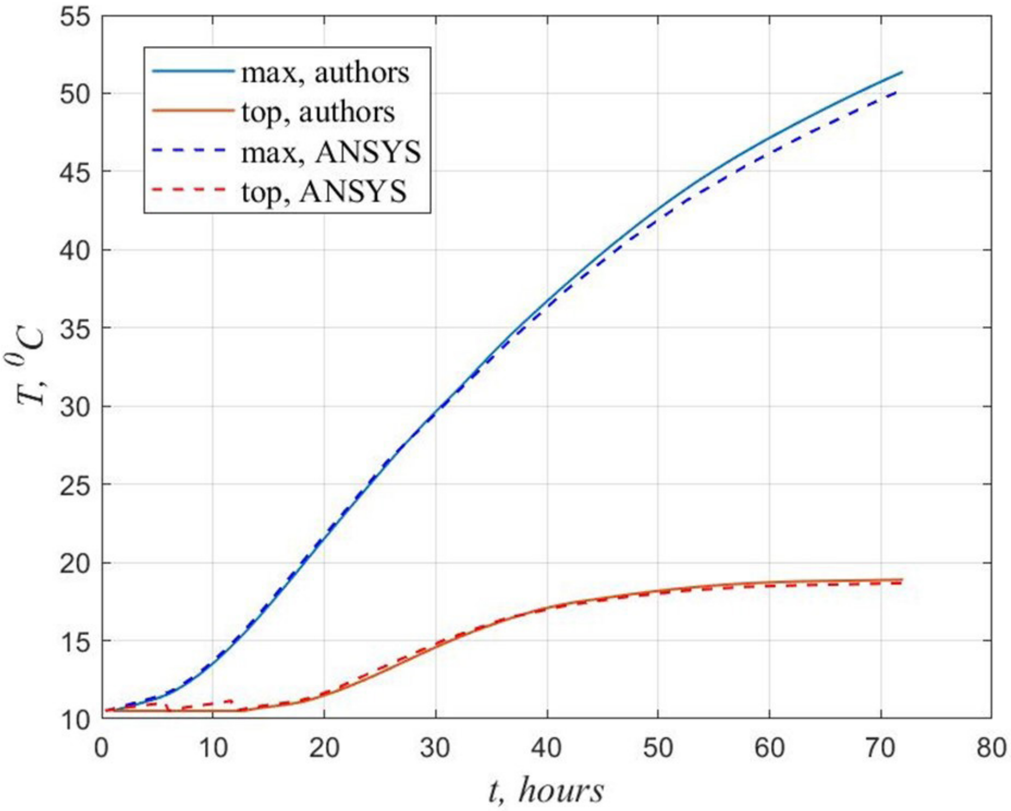

Fig. 10. Comparison of the solution with the results in the ANSYS software

The calculations described above assumed that the structures are made in one step, i.e., stages of construction were not considered. In the program that we developed earlier, this circumstance can be easily considered by adding new finite elements in concreting. This option is also available in the ANSYS software and is called “Element Birth and Death”.

Let us provide an example for the analysis of a foundation slab with dimensions of 10 × 10 × 2 m. The structure is concreted in three layers with a thickness of 0.667 m. The pauses (breaks) in concreting in layers t_{br} varied from 0 to 12 hours. For simplicity, the soil temperature, the initial temperature of the concrete mix, and the environmental temperature were taken constant and equal to 10.5°C. The coefficient of heat transfer between the environment and the top surface h_1 = 25 W/(m^2×°C). The composition of concrete corresponds to composition 1 in Fig. 2.

Fig. 9 presents changes in the maximum temperature difference at different t_{br} values. It shows that pauses (breaks) in concreting in layers make it possible to reduce the maximum temperature difference but not so significantly. It is more efficient to use concretes characterized by low heat release and control heat exchange conditions on the top surface.

To ensure the validity of the results, we compared the solution with the ANSYS software results at 6-hour pauses (breaks) in concreting in layers. Fig. 10 shows a comparison of the maximum temperatures in the foundation and the temperatures on the top surface, obtained using the program that we developed earlier and ANSYS. Fig. 11 shows the temperature distribution obtained with the use of ANSYS at t = 72 h. The discrepancy between the results is insignificant.

Discussion

Based on the parametric studies, we established that the most significant factors affecting the temperature difference between the center and the surface of the structure of mass foundation slabs are heat exchange conditions on the top surface, structural thickness, and the heat release rate. The need for heat insulation of the top surface immediately after concreting is finished was previously addressed by Korotchenko et al. (2016), Nguyen and Luu (2019), and others.

The results of numerical modeling at different ratios between the thickness of the foundation slab H_F and its dimensions in plan a show that, already at $a/H_F>=4$, the temperature distribution through the thickness in the middle part of the foundation, when the problem is solved in a three-dimensional formulation, coincides with the distribution from the solution of a one-dimensional problem. For instance, a structure with dimensions of 2.8 × 2.8 × 0.7 m will have the same risk of early cracking as a structure with dimensions of 28 × 28 × 0.7 m. Besides, the use of a one-dimensional formulation significantly saves computing time when selecting the optimal construction conditions.

The calculation of temperature fields with account for the layer-by-layer concreting with pauses (breaks) showed that such pauses in concreting in layers make it possible to reduce the temperature difference between the center and the surface of the structure but not so significantly. Meanwhile, these pauses should have a sufficient duration.

In the examples considered, the thermophysical

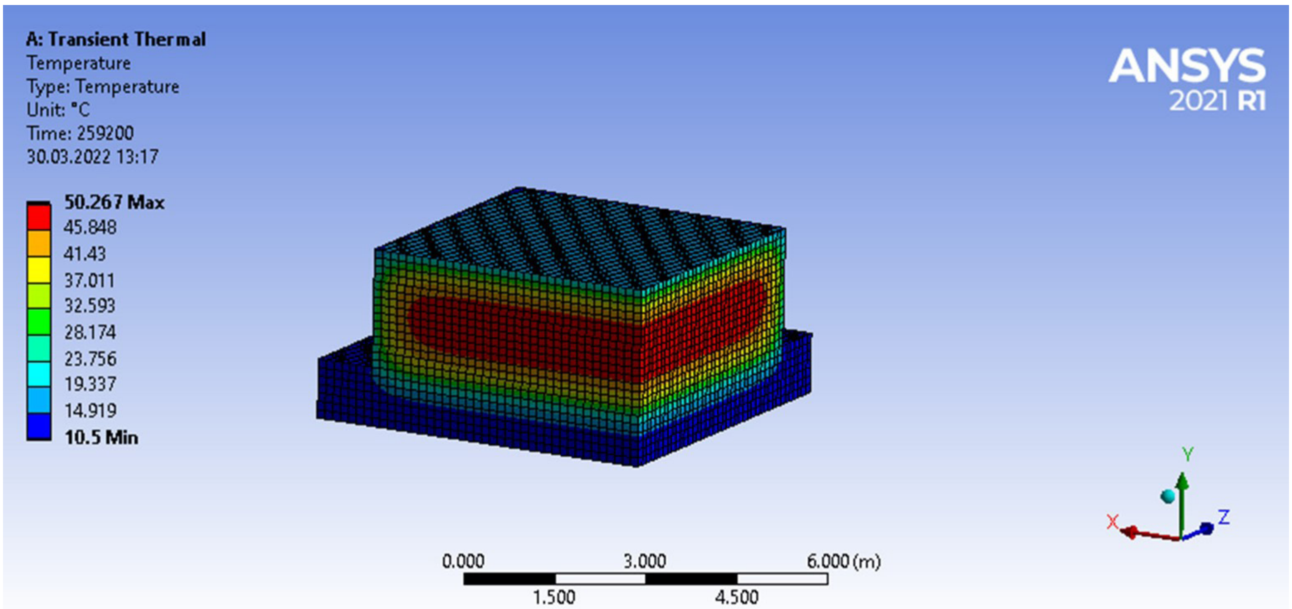

Fig. 11. Temperature distribution in the ANSYS software at t = 72 h

properties of concrete were taken constant in time. In the program that we developed earlier, the thermal conductivity coefficient and heat capacity of concrete vs. time relationships can be easily considered (in contrast to the existing software (ANSYS, Abaqus, etc.)), but reliable experimental data are required.

It should be noted that the conclusions above were drawn from the perspective of minimizing the temperature difference between the center and the surface of the structure, which allows us to estimate thermal stresses arising in the structure only indirectly. To obtain a complete picture of the risk of early cracking, it is necessary to perform a stress-strain state analysis based on the obtained temperature fields. In this case, such factors as changes in the mechanical characteristics of concrete in time, creep and chemical shrinkage as well as the reinforcement ratio should be considered. Besides, during stress-strain state analysis, it is also required to apply the analysis of the influence of construction stages, which we performed when calculating the temperature fields. This will be the focus of our further research.

Conclusions

In the course of the study, we developed a mathematical model to calculate temperature fields that arise during the manufacturing of mass cast-in-situ foundation slabs. The novelty of the proposed model is that it takes into account the influence of construction stages on the resulting temperature fields. We applied finite element modeling in one-dimensional and three-dimensional cases using the software that we developed earlier. Verification and validation of the model were performed based on experimental data and by comparing it with a numerical solution in the ANSYS software. It was shown that the discrepancy between the solution obtained and experimental data as well as the results of the numerical analysis in the ANSYS environment does not exceed 5%. We also performed a parametric study to determine how such factors as the ratio of dimensions, heat transfer conditions on the surfaces, concrete recipe, pauses during concreting and their duration affect the maximum temperature difference between the center and the surface of the structure. As a result, we established that the most significant risk factors for early cracking are heat exchange conditions on the top surface, structural thickness, and the heat release rate.

References

Abeka, H., Agyeman, S., and Adom-Asamoah, M. (2017). Thermal effect of mass concrete structures in the tropics: Experimental, modelling and parametric studies. *Cogent Engineering*, Vol. 4, Issue 1, 1278297. DOI: 10.1080/23311916.2016.1278297.

Aniskin, N. and Nguyen, T.-C. (2019). Influence factors on the temperature field in a mass concrete. *E3S Web of Conferences*, Vol. 97, 05021. DOI: 10.1051/e3sconf/20199705021.

Bofang, Z. (2014). *Thermal stresses and temperature control of mass concrete.* Oxford: Butterworth-Heinemann, 500 p. DOI*: 10.1016/C2012-0-06038-3.*

Castilho, E., Schclar, N., Tiago, C., and Farinha, M. L. B. (2018). FEA model for the simulation of the hydration process and temperature evolution during the concreting of an arch dam. *Engineering Structures*, Vol. 174, pp. 165–177. DOI: 10.1016/j.engstruct.2018.07.065.

Chuc, N. T., Le, Q. D., Thoan, P. V., and Kiet, B. A. (2018). The effects of insulation thickness on temperature field and evaluating cracking in the mass concrete. *Electronic Journal of Structural Engineering*, Vol. 18, No. 2, pp. 128–132.

Długosz, A., Pokorska, I., Glinicki, M. A., and Jaskulski, R. (2017). Identification of thermal properties of hardening concrete by means of evolutionary algorithms. *Computer Assisted Methods in Engineering and Science*, Vol. 24, No. 2, pp. 101–111. DOI: 10.24423/cames.208.

Fairbairn, E. M. R., Silvoso, M. M., Toledo Filho, R. D., Alves, J. L. D., and Ebecken, N. F. F. (2004). Optimization of mass concrete construction using genetic algorithms. *Computers & Structures*, Vol. 82, Issues 2–3, pp. 281–299. DOI: 10.1016/j.compstruc.2003.08.008.

Havlásek, P., Šmilauer, V., Hájková, K., and Baquerizo, L. (2017). Thermo-mechanical simulations of early-age concrete cracking with durability predictions. *IOP Conference Series: Materials Science and Engineering*, Vol. 236, 012052. DOI: 10.1088/1757-899X/236/1/012052.

Javanmardi, F. and Léger, P. (2005). Grouting of cracks in concrete dams: numerical modelling and structural behavior. *Progress in Structural Engineering and Materials*, Vol. 7, Issue 4, pp. 161–173. DOI: 10.1002/pse.201.

Klemczak, B., Batog, M., Pilch, M., and Żmij, A. (2017). Analysis of cracking risk in early age mass concrete with different aggregate types. *Procedia Engineering*, Vol. 193, pp. 234–241. DOI: 10.1016/j.proeng.2017.06.209.

Klemczak, B. and Knoppik-Wróbel, A. (2011). Early age thermal and shrinkage cracks in concrete structures – description of the problem. *Architecture, Civil Engineering, Environment*, Vol. 4, No. 2, pp. 35–48.

Korotchenko, I., Ivanov, E., Semenov, K., and Barabanshchikov, Y. (2016). Thermal stressed state in massive concrete structures in the winter building period. *MATEC Web of Conferences,* Vol. 53, 01001. DOI: 10.1051/matecconf/20165301001.

Kuriakose, B., Nageswara Rao, B., and Dodagoudar, G. R. (2016). Early-age temperature distribution in a massive concrete foundation. *Procedia Technology*, Vol. 25, pp. 107–114. DOI: 10.1016/j.protcy.2016.08.087.

Kuryłowicz-Cudowska, A. (2019). Determination of thermophysical parameters involved in the numerical model to predict the temperature field of cast-in-place concrete bridge deck. *Materials*, Vol. 12, Issue 19, 3089. DOI: 10.3390/ma12193089.

Lukyanov, V. S. (1935). *Hydraulic models for solving problems of heating and cooling solids and propagation in thermal systems. Patent SU45112A1*.

Nguyen, T.-C., Huynh, T.-P., and Tang, V.-L. (2019). Prevention of crack formation in massive concrete at an early age by cooling pipe system. *Asian Journal of Civil Engineering*, Vol. 20, Issue 8, pp. 1101–1107. DOI: 10.1007/s42107-019-00175-5.

Nguyen, T.-C. and Luu, X. B. (2019). Reducing temperature difference in mass concrete by surface insulation. *Magazine of Civil Engineering***,** No. 88 (4), pp. 70–79. DOI: 10.18720/MCE.88.7.

Rahimi, A. and Noorzaei, J. (2011). Thermal and structural analysis of roller compacted concrete (R.C.C) dams by finite element code. *Australian Journal of Basic and Applied Sciences*, Vol. 5, Issue 12, pp. 2761–2767.

Segerlind, L. J. (1984). *Applied finite element analysis*. 2nd edition. New York: Willey, 427 p.

Semenov, K., Kukolev, M., Zaichenko, N., Popkov, S., Makeeva, A., Amelina, A. and Amelin, P. (2019). Unsteady temperature fields in the calculation of crack resistance of massive foundation slab during the building period. In: Borodinecs, A., Vatin, N., and Sergeev, V. (eds.) *Proceedings of EECE 2019*, Vol. 70. Cham: Springer, pp. 455–467. DOI: 10.1007/978-3-030-42351-3_40.

Tasri, A. and Susilawati, A. (2019). Effect of material of post-cooling pipes on temperature and thermal stress in mass concrete. *Structures*, Vol. 20, pp. 204–212. DOI: 10.1016/j.istruc.2019.03.015.

Van Breugel, K. (1998). Prediction of temperature development in hardening concrete. In: Springenschmid, R. (ed.) *Prevention of thermal cracking in concrete at early ages*. London: CRC Press, pp. 51–75.

Van Lam, T., Nguen, C. C., Bulgakov, B. I., and Anh, P. N. (2018). Composition calculation and cracking estimation of concrete at early ages. *Magazine of Civil Engineering*, No. 6 (82), pp. 136–148. DOI: 10.18720/MCE.82.13.

Xie, Z., Wang, L., Zhu, Z., Fu, Z., and Lv, X. (2020). Simulation of the temperature field for massive concrete structures using an interval finite element method. *Engineering Computations*, Vol. 37, Issue 7, pp. 2467–2486. DOI: 10.1108/EC-10-2019-0456.

Xu, J., Shen, Z., Yang, S., Xie, X., and Yang, Z. (2019). Finite element simulation of prevention thermal cracking in mass concrete. *International Journal of Computing Science and Mathematics*, Vol. 10, No. 4, pp. 327–339. DOI: 10.1504/IJCSM.2019.102691.

Zhang, M., Yao, X., Guan, J., and Li, L. (2020). Study on temperature field massive concrete in early age based on temperature influence factor. *Advances in Civil Engineering*, Vol. 2020, 8878974. DOI: 10.1155/2020/8878974.

МОДЕЛИРОВАНИЕ НЕСТАЦИОНАРНЫХ ТЕМПЕРАТУРНЫХ ПОЛЕЙ ПРИ ВОЗВЕДЕНИИ МАССИВНЫХ МОНОЛИТНЫХ ЖЕЛЕЗОБЕТОННЫХ ФУНДАМЕНТНЫХ ПЛИТ

Антон Сергеевич Чепурненко*, Григорий Васильевич Несветаев, Юлия Игоревна Корянова

Донской государственный технический университет
Площадь Гагарина 1, Ростов-на-Дону, Россия

*E-mail: anton_chepurnenk@mail.ru

Аннотация

Для массивных монолитных железобетонных конструкций за счет внутреннего тепловыделения бетона и теплообмена с окружающей средой при твердении происходит неравномерный нагрев, что может привести к раннему трещинообразованию и невозможности дальнейшей эксплуатации конструкций. Одним из основных факторов, предопределяющих риск раннего трещинообразования, является перепад температур между центром и поверхностью конструкции. **Целью работы** является анализ влияния на величину максимального перепада температур между серединой и поверхностью конструкции таких факторов, как соотношение габаритов конструкции, условия теплопередачи на поверхностях, рецептура бетона, наличие и величина технологических перерывов. **Использованы следующие методы**: Конечно-элементное моделирование в трехмерной и одномерной постановке с использованием разработанного авторами программного обеспечения в среде MATLAB. **В результате** установлено, что факторами, в большей степени влияющими на риск раннего трещинообразования, являются условия теплообмена на верхней поверхности, толщина конструкции и плотность внутреннего тепловыделения бетона. Верификация и валидация модели выполнена на экспериментальных данных, а также путем сравнения с численным решением в программном комплексе ANSYS.

Ключевые слова

Массивные железобетонные конструкции, фундаментная плита, трещинообразование, температурное поле, метод конечных элементов, внутренние источники тепловыделения.